
Structure and ion channel activity of the human respiratory syncytial virus (hRSV) small hydrophobic protein transmembrane domain

SIOK WAN GAN, LIFANG NG, XIN LIN, XIANDI GONG, AND JAUME TORRES

School of Biological Sciences, Nanyang Technological University, 637551 Singapore

(RECEIVED November 22, 2007; FINAL REVISION January 21, 2008; ACCEPTED January 21, 2008)

Abstract

The small hydrophobic (SH) protein from the human respiratory syncytial virus (hRSV) is a glycoprotein of ~64 amino acids with one putative α -helical transmembrane domain. Although SH protein is important for viral infectivity, its exact role during viral infection is not clear. Herein, we have studied the secondary structure, orientation, and oligomerization of the transmembrane domain of SH (SH-TM) in the presence of lipid bilayers. Only one oligomer, a pentamer, was observed in PFO-PAGE. Using polarized attenuated total reflection-Fourier transform infrared (PATR-FTIR) spectroscopy, we show that the SH-TM is α -helical. The rotational orientation of SH-TM was determined by site-specific infrared dichroism (SSID) at two consecutive isotopically labeled residues. This orientation is consistent with that of an evolutionary conserved pentameric model obtained from a global search protocol using 13 homologous sequences of RSV. Conductance studies of SH-TM indicate ion channel activity, which is cation selective, and inactive below the predicted pK_a of histidine. Thus, our results provide experimental evidence that the transmembrane domain of SH protein forms pentameric α -helical bundles that form cation-selective ion channels in planar lipid bilayers. We provide a model for this pore, which should be useful in mutagenesis studies to elucidate its role during the virus cycle.

Keywords: small hydrophobic protein; ion channel; infrared dichroism; molecular dynamics

The small hydrophobic (SH) protein is a transmembrane surface glycoprotein encoded by the human respiratory syncytial virus (hRSV). During infection, the majority of the SH protein accumulates at the lipid-raft structures of the Golgi complex (Rixon et al. 2004), and also at the cell

surface. Only a very low amount of SH protein is associated with the viral envelope (Rixon et al. 2004). SH is categorized as an accessory protein of hRSV, as it is not essential for viral replication in vitro (Bukreyev et al. 1997). However, deletion of the SH gene leads to attenuation in mouse and chimpanzee models, suggesting it is important for infectivity (Bukreyev et al. 1997; Whitehead et al. 1999).

The SH protein is 64–65 amino acids long, depending on the viral strain; 64 amino acids are found in subgroup A and 65 amino acids in subgroup B. Biochemical studies have shown that the SH protein has a single hydrophobic region that spans the membrane, with the more hydrophilic C terminus oriented extracellularly (Collins and Mottet 1993). Several forms of SH protein are present during infection, which vary in their glycosylation status (Olmsted and Collins 1989): two not glycosylated forms, full-length 7.5 kDa (SH₀) and a truncated 4.5-kDa

Reprint requests to: Jaume Torres, School of Biological Sciences, Nanyang Technological University, 60, Nanyang Drive, 637551 Singapore; e-mail: jtorres@ntu.edu.sg; fax: 65-6791-3856.

Abbreviations: PFO-PAGE, perfluorooctanoate-polyacrylamide gel electrophoresis; SDS-PAGE, sodium dodecyl sulfate-polyacrylamide gel electrophoresis; TMHMM, Transmembrane Hidden Markov Model; NCBI, National Center for Biotechnology Information; RMSD, root mean square deviation; GSMD, global search molecular dynamics; DMPC, dimyristoyl-phosphatidylcholine; POPC, 1-palmitoyl-2-oleoyl-sn-glycero-3-phosphatidylcholine; POPE, 1-palmitoyl-2-oleoyl-sn-glycero-3-phosphatidylethanol; POPS, 1-palmitoyl-2-oleoyl-sn-glycero-3-phosphatidylserine.

Article published online ahead of print. Article and publication date are at <http://www.proteinscience.org/cgi/doi/10.1110/ps.073366208>.

species (SH_t), an N-linked glycosylated form (SH_g), and a polylactosaminoglycan-modified form (SH_p). All, except the truncated SH_t, are incorporated at the surface of the infected cells, where non-glycosylated SH₀ appears to be the most abundant form (Collins and Mottet 1993). In addition to these modifications, the tyrosine residues of SH protein are phosphorylated during infection, and this modification affects its cellular distribution (Rixon et al. 2005).

Although the role played by the SH protein during viral infection is currently unknown, some studies suggest an ancillary role in virus-mediated cell fusion (Heminway et al. 1994; Techaarpornkul et al. 2001). More recently, cell studies have suggested that SH protein can inhibit apoptosis in several mammalian cell lines by evading the host immune response (Fuentes et al. 2007).

In addition to the above, it has been suggested that SH could form ion channels, because SH protein expressed in *Escherichia coli* can modify the permeability of the bacterial membrane to low-molecular-weight compounds (Perez et al. 1997). Also, in SDS, cross-linking of SH protein generated at least four oligomers that include dimers, trimers, tetramers, and pentamers (Collins and Mottet 1993; Rixon et al. 2005). Thus, SH protein has been predicted to be a viroporin, a group of small, highly hydrophobic virus proteins that can oligomerize and form pores at the cell membrane (Gonzalez and Carrasco 2003).

Herein, we have examined this hypothesis by determining the SH-TM oligomeric state and structure using experimental and computational approaches. We have obtained the oligomeric size using detergents and a global search of helix-helix interactions using homologous sequences (Briggs et al. 2001). The latter approach requires an exhaustive conformational search, with a grid of initial configurations; conservative mutations that appeared during evolution acted as a filter for nonnative models. This procedure allows us to define not only conserved interactions, but also oligomeric size (Torres et al. 2000, 2002, 2005; Lin et al. 2006; Gan et al. 2007). The orientation of the individual α -helices of SH-TM in lipid bilayers has been obtained using site-specific infrared dichroism (Arkin et al. 1997) of isotopically labeled peptides with a $^{13}\text{C}=^{18}\text{O}$ peptidic carbonyl (Torres et al. 2000, 2001b). Finally, we have performed conductance studies in planar lipid bilayers to test if SH-TM can form ion channels.

Results

Gel electrophoresis

To test our hypothesis that SH-TM oligomerize in lipid bilayers, we performed electrophoreses of this peptide in two different environments. Figure 1 shows gel electrophoreses of SH-TM in SDS and the milder PFO. Whereas

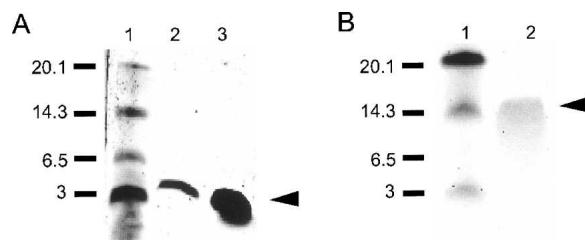


Figure 1. PAGE analysis of SH-TM. (A) Electrophoresis in SDS. In lane 2, the peptide was loaded without previous heating. In lane 3, the sample was boiled for 5 min. (B) Electrophoresis in PFO. In lane 2, the sample was boiled for 5 min before loading. The arrows indicate the bands consistent with monomer in SDS (A) or pentamer in PFO (B). Lane 1 in both gels corresponds to the molecular weight markers. Molecular masses are indicated (in kilodaltons).

only one band consistent with SH-TM monomers (2.98 kDa) is observed in SDS (Fig. 1A), an ~ 15 kDa band consistent with a pentamer is clearly observed in PFO (Fig. 1B).

Conformational search for RSV TM homo-pentamers

A global search (see Materials and Methods) was performed using the predicted transmembrane domain of SH protein and its homologous sequences (see Fig. 2). During the simulations, a pentameric size was assumed, following the result shown in Figure 1B. Structures shared by all RSV sequences, and hence evolutionarily conserved, were only observed when the helix tilt was restrained to 25° . Only two complete sets were found (Fig. 2, lower panel), which were left-handed structures. The C α RMSD between any pair of structures within these “complete sets” was never higher than 1.2 Å. No other complete sets were found for other helix tilts.

In model 1, the rotational orientation ω (Arkin et al. 1997) for residue 30 (ω_{30}) was 130° , whereas in model 2, ω_{30} was 240° , i.e., a difference of 110° . The helix tilt was 25° and 20° , respectively. Representative structures for these two sets are shown in Figure 2, lower panel.

Infrared dichroic data

To determine which one of these two models is correct, we measured the rotational orientation of SH-TM α -helices in model lipid bilayers (DMPC) shown in Figure 3. Both the frequencies of amide A (Fig. 3A,C), at 3305 cm^{-1} , and amide I (Fig. 3B,D), centered at 1653 cm^{-1} , are consistent with an α -helical conformation (Byler and Susi 1986). In the peptide labeled at L30, the band corresponding to the isotopic $^{13}\text{C}=^{18}\text{O}$ label is centered at 1592 cm^{-1} (Fig. 3B, arrow), as expected for a residue in an α -helical conformation (Torres et al. 2001b). For the peptide labeled at residue L31, however, this band

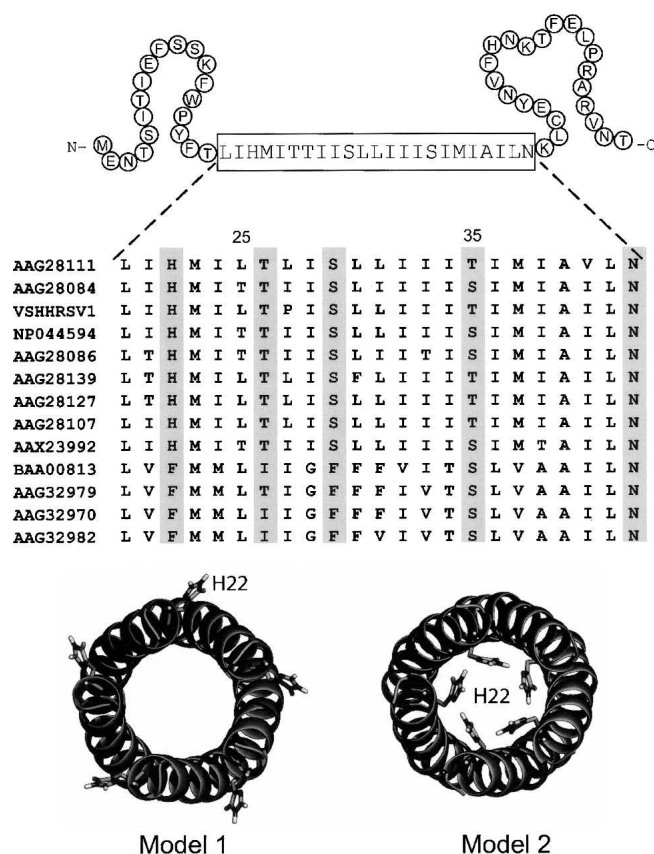


Figure 2. The sequence of SH protein and evolutionarily conserved pentameric models. (Upper panel) Schematic representation of the full-length sequence of SH protein from hRSV subgroup A. The predicted transmembrane domain (see Materials and Methods) is boxed. Sequences corresponding to SH-TM homologs used in our molecular dynamics simulations are shown, with conserved polar residues in gray. The NCBI entries are indicated on the left column. The first nine sequences are from various subtypes of hRSV, and the last four sequences are from bovine RSV variants. The numbering shown at the top corresponds to the full-length protein. (Lower panel) Top view of the two pentameric evolutionarily conserved models obtained from the global search. Residue H22 is shown in a stick representation.

appeared at a lower frequency, 1576 cm^{-1} (Fig. 3D, arrow). As this band is not obscured by either amide I or II, and is well resolved (see Fig. 3D), this shift did not affect the measurement. The down-shift of the frequency of this band, relative to L30, is explained in the Discussion section. The dichroic ratios obtained for each label in DMPC are listed in Table 1. Using the equations for SSID described in Materials and Methods (Arkin et al. 1997), we obtained an average ω_{30} of $258^\circ (\pm 7.3^\circ)$. This orientation is only consistent with that of model 2 (Fig. 2, lower panel), which is 240° . The helix tilt obtained from SSID was $21.5^\circ (\pm 1.3^\circ)$, which is also similar to that of model 2. The fractional order parameter (Arkin et al. 1997), f , was around 0.5. Slices through the pentameric model 2 are presented in Figure 4.

Although these FTIR measurements were performed at room temperature, the frequency of the lipid methylene C–H stretching bands indicated that DMPC ($T_m = 23^\circ\text{C}$) was in the gel phase (Tamm and Tatulian 1997). Therefore, we repeated these infrared measurements in POPC ($T_m = -2^\circ\text{C}$), which should form a fluid liquid crystal phase. This was indeed observed by a shift of the lipid symmetric methylene stretching vibration, from 2849 cm^{-1} to 2852 cm^{-1} , and the anti-symmetric methylene stretching vibration, from 2917 cm^{-1} to 2922 cm^{-1} (not shown) (Tamm and Tatulian 1997). With the data obtained in POPC, we calculated ω_{30} to be $271^\circ (\pm 16.0^\circ)$ and the helix tilt β of $30^\circ (\pm 3.4^\circ)$, in good agreement with the result obtained in DMPC.

Cation selectivity

To test the hypothesis that SH-TM has ion channel activity, we reconstituted SH-TM in black lipid membranes. The current traces are shown in Figure 5A, which show current reversal at approximately -60 mV . From the linear current–voltage plots shown in Figure 5B, we calculated a conductance of $\sim 35\text{ pS}$, and -68.1 mV for the reversal potential, close to the sodium Nernst potential in our experiment (-59.1 mV), indicating that the channel is cation selective. At voltages below and above the reversal potential, the channel activities were similar

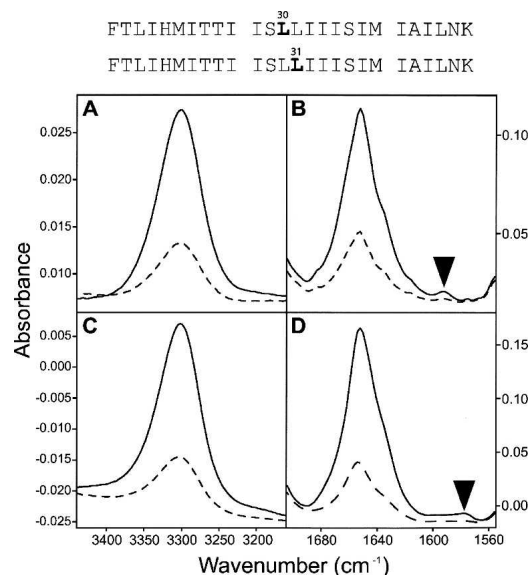


Figure 3. Polarized ATR-FTIR absorbance spectra of SH-TM reconstituted in DMPC bilayers. (A) Amide A region of L30; (B) amide I region of L30. The position of the labeled C=O stretching band is indicated with an arrow. Solid lines and broken lines indicate spectra obtained at parallel or perpendicular polarization, respectively. (C,D) The scenario is the same for L31. The sequence of synthetic SH-TM, with the position of the two consecutive labels are shown at the top.

Table 1. Dichroic ratios measured by SSID using the amide A and the isotopic label bands for SH-TM incorporated in DMPC and POPC lipid bilayers

Measurements	L30		L31	
	R_{helix}	R_{site}	R_{helix}	R_{site}
DMPC				
<i>a</i>	3.0	2.2	3.2	4.3
<i>b</i>	3.4	2.5	3.5	5.2
<i>c</i>	3.0	2.4	3.6	6.2
POPC				
<i>a</i>	2.7	2.5	3.1	7.5
<i>b</i>	2.7	2.4	3.0	4.5
<i>c</i>	2.6	2.0	2.7	4.3

(Fig. 5C), suggesting a voltage-independent opening probability.

Histidine is the only protonatable residue in the SH-TM (Fig. 2). In model 1 (Fig. 2) the histidine is facing the lipid acyl chains, whereas in model 2 it is facing the lumen of the pore. To confirm our SSID results that point to model 2, we tested the effect of pH on the conductance observed. Thus, we measured the ion channel activity at a pH below (4.0) and above (7.4) the expected pK_a of histidine in these conditions. In the bulk, the expected pK_a of histidine imidazole is 6.4 (Cymes et al. 2005), whereas in the tetrameric pore of M2 from influenza A, this value was determined to be ~ 5.8 (#5100) (Okada

et al. 2001). Figure 5D shows a much lower conductance at pH 4.0, and the current has the opposite sign. This strong pH dependence confirms that His must be exposed to the lumen of the pore, as in model 2.

Discussion

The role played by SH protein during virus infection is currently unknown. Specifically, its possible ion channel activity has not been investigated. We provide experimental evidence that the transmembrane domain of SH protein forms pentameric α -helical bundles that form cation-selective ion channels in planar lipid bilayers.

Our results in the harsh detergent SDS, where we only observe SH-TM monomers, are consistent with the fact that higher oligomers of SH could only be observed in SDS after cross-linking (Collins and Mottet 1993). In PFO, in contrast, we observe only one oligomeric band, corresponding to pentamers. PFO is a mild detergent that can provide the conditions for stable native interactions between transmembrane α -helices (Ramjeesingh et al. 1999) and has been applied to various transmembrane peptides to identify their true oligomeric size (Therien and Deber 2002; Beevers and Kukol 2006).

Our conformational search yielded two evolutionarily conserved pentameric models, both left-handed (Fig. 2, lower panel). We note that in a similar computational study (Kochva et al. 2003), a model was proposed that

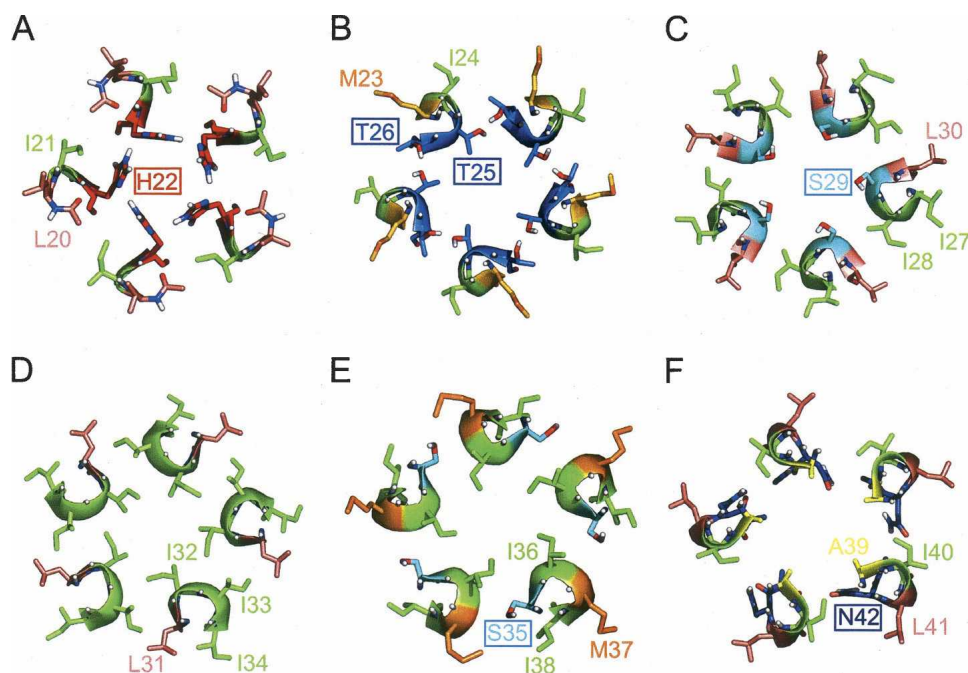


Figure 4. Consecutive slices corresponding to model 2 in Figure 2. Residues 20–22 (A), 23–26 (B), 27–30 (C), 31–34 (D), 35–38 (E), and 39–42 (F). The residue numbers are indicated and polar residues are boxed. Color code: I, green; L, salmon; T, marine; S, cyan; M, orange; H, red; A, yellow; and N, blue.

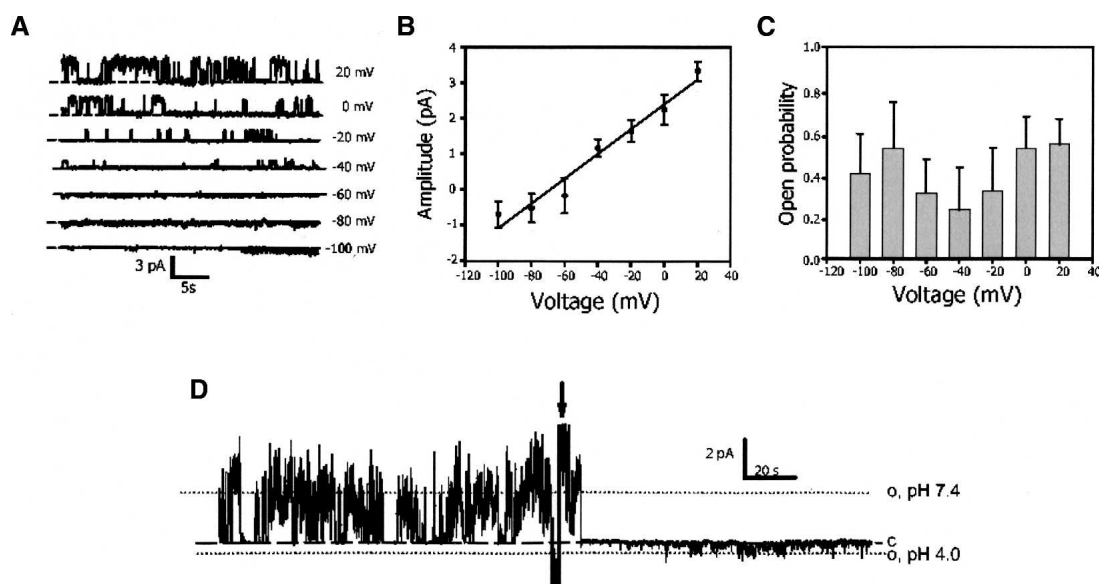


Figure 5. Single channel activity observed for SH-TM. (A) Single channel currents recorded over a range of membrane potentials indicated on the right, with openings shown as deviations from the baseline (dashed line). (B) Current–voltage relationship for open state of the channel. (C) The variation of open probability of the channel at different potential. (B,C) Mean of data from three to five recordings. (D) Single channel currents at pH 7.4 and pH 4.0 when the bilayer membrane potential was held at +60 mV. The arrow indicates the change from pH 7.4 to pH 4.0.

was consistent with the model 1 in Figure 2. However, in Kochva's work (Kochva et al. 2003), the helix tilt was not restrained, whereas our simulations were performed after restraining the helix tilt every 10°, from 5° to 45°. Restraining the helix tilt ensures that all conformational space is explored, as we have shown previously for influenza A M2 (Torres et al. 2001a), where an evolutionarily conserved model showing the correct helix–helix interactions and helix tilt was only found when the tilt was restrained to 30°, but not when the helix tilt was not restrained. In addition, only model 2 is consistent both with our experimental SSID results and with the observed strong pH dependence of the conductance.

In model 2, H22 is facing the lumen of the pore, which is reminiscent of the orientation of H37 in influenza A M2 (Kovacs and Cross 1997). However, whereas M2 becomes open at low pH, below the pK_a of histidine (Okada et al. 2001), we observed that conductance of SH-TM is reduced drastically from pH 7.4 to 4. This suggests that histidine protonation stops cation transport due to an electrostatic effect. A small opposite conductance is observed at pH 4.0, which could indicate chloride transport.

Neither of the conserved polar residues of SH-TM: T26, S29, T/S35, and N42 (highlighted in the sequence alignment in Fig. 2), are facing the acyl chains of the lipids (Fig. 4; see boxed residues). Thus, these polar residues may be involved in ion channel selectivity or in interhelical interactions, as observed in other transmembrane systems (Gratkowski et al. 2001; Smith et al. 2002).

Future mutagenesis work will determine the precise role of these residues.

In our infrared spectra, we have observed a shift in the isotopically labeled $^{13}\text{C}=^{18}\text{O}$ band for residue L31, from 1592 cm^{-1} to a much lower frequency, 1576 cm^{-1} . We attribute this shift to the presence of an extra hydrogen bond with another side chain group or solvent, which has the effect of weakening the $\text{C}=\text{O}$ bond. Indeed, the α -helical model of SH-TM is compatible with an intrahelical hydrogen bond between the side chain of S35 and the backbone carbonyl oxygen of L31 (Fig. 6). There is a high tendency for serine and threonine residues to form intrahelical hydrogen bonds to carbonyl oxygen at position $i-4$ (Baker and Hubbard 1984), and to our knowledge, this is the first instance of such spectral effect observed. Statistical studies of high resolution structures of several membrane proteins and soluble proteins have suggested

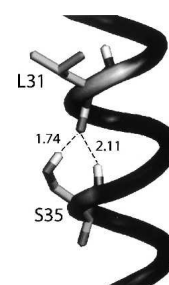


Figure 6. The hydrogen bonding between S35 and L31.

that intrahelical hydrogen bonding between the side chain of serine or threonine *to the carbonyl oxygen in the preceding turn* could induce a kink in the α -helix that may be important for function (Ballesteros et al. 2000). We are at present studying the relevance of this interaction in the channel properties of SH.

Recently, studies have indicated that SH protein can inhibit apoptosis in several mammalian cell lines by blocking the tumor necrosis factor alpha (TNF- α)-mediated apoptotic signaling pathway (Fuentes et al. 2007). However, ion channels may also control apoptosis in cells (Szabo et al. 2004; Lang et al. 2005; Burg et al. 2006). Inhibition of apoptosis in host cells during infection gives an advantage to the virus to replicate. Amantadine, a drug that blocks the ion channel of several viroporins (Duff and Ashley 1992; Skehel 1992; Griffin et al. 2003; Torres et al. 2007) could be used to obtain further understanding of the channel properties of SH protein.

Materials and Methods

Peptide purification

Synthetic peptides, 26 residues long, corresponding to the transmembrane segment of SH (residues 18–43) were obtained by microwave assisted solid-phase fluorenylmethyloxycarbonyl (Fmoc) chemistry using the Odyssey Microwave peptide synthesizer (CEM Corporation). The peptides were prepared on a 0.025-mmol scale with acetylated N terminus and amidated C terminus, cleaved from the resin with trifluoroacetic acid (TFA) and lyophilized. Two peptides were synthesized corresponding to the sequence shown in Figure 3 (top), each containing one $^{13}\text{C}=\text{O}$ -labeled carbonyl at positions L30 or L31.

The lyophilized peptides were dissolved in a minimum amount of TFA (<10 μL) followed by dilution to 1 mL of acetonitrile to a final peptide concentration of ~ 5 mg/mL and immediately injected onto a Zorbax C18–300 Å column (Phenomenex) connected to a high-performance liquid chromatography (HPLC) system (Shimadzu). The solvents used were solvent A (water/TFA, 99.9:0.1, v/v) and solvent D (isopropanol/acetonitrile/TFA, 80:19.9:0.1, v/v). The column was previously equilibrated with a mixture of solvents A and D (7:3, v/v). The peptide was eluted with a linear gradient to a final solvent composition of 75% of solvent D. Pooled fractions were lyophilized and the purity of the samples was checked by electrospray ionization mass spectrometry (ESI-MS), which did not show the presence of adducts (data not shown).

$^{16}\text{O}/^{18}\text{O}$ exchange

The exchange of $^{13}\text{C}=\text{O}$ to $^{13}\text{C}=\text{O}$ was performed as described previously (Torres et al. 2000). Briefly, the two oxygen atoms in the carboxylic group of $^{13}\text{C}=\text{O}$ -labeled leucine (Cambridge Isotopes Laboratories) were exchanged to ^{18}O by incubating the amino acid at 100°C at acidic pH conditions (pH ~ 1) with a mixture of H_2^{18}O and dioxane (3:1, v/v) for 1 h. The extent of exchange was monitored using mass spectrometry. The solution was lyophilized and the amino

acid was derivatized with Fmoc as described (Wellings and Atherton 1997).

Gel electrophoresis

The peptide sample was subjected to reduced SDS-PAGE or PFO-PAGE using precast tricine gradient gel (Bio-rad), with or without heat treatment. SDS or PFO sample buffer was added to the lyophilized peptide to a final concentration of 2 $\mu\text{g}/\mu\text{L}$. The sample was mixed with sample buffer for 1 min followed by heating at 95°C for 5 min before loading to the gel. The gel was run at constant voltage of 80 V for 3 h at room temperature. The molecular mass markers were obtained from Bio-Rad. The gel was stained with Coomassie blue.

Infrared spectroscopy

FTIR spectra were recorded on a Nicolet Nexus 560 spectrometer purged with N_2 and equipped with a MCT/A detector cooled with liquid nitrogen. Attenuated total reflection (ATR) spectra were measured with a 25-reflections ATR accessory from Graseby Specac and a wire grid polarizer (0.25 mM, Graseby Specac). Approximately 100 μL of sample in water with a 20:1 lipid/peptide molar ratio were applied onto a trapezoidal (50 mm \times 2 mm \times 20 mm) Ge internal reflection element. The lipid used here was DMPC and POPC (Avanti Polar Lipids). A dry or $^2\text{H}_2\text{O}$ saturated N_2 stream flowing through the ATR compartment was used to remove bulk water or to achieve $^2\text{H}_2\text{O}$ exchange, respectively. After insertion of the plate in the ATR cell, spectra were collected. A total of 200 interferograms collected at a resolution of 4 cm^{-1} were averaged for every sample and processed with 1.0 filling and Happ-Genzel apodization. The area corresponding to the $^{13}\text{C}=\text{O}$ (isotope-labeled) carbonyl stretching vibration was obtained integrating the band at 1590 cm^{-1} . The area of the amide A (N–H stretching, centered at ~ 3300 cm^{-1}) was obtained by peak integration from 3200 cm^{-1} to 3400 cm^{-1} . No difference in band area was observed employing other means of peak size estimation such as peak fitting and Fourier self-deconvolution. The helix dichroism was measured from the amide A when the sample was hydrated in $^2\text{H}_2\text{O}$. The dichroic ratio of the band was calculated as the ratio between the integrated absorptions of the spectra collected with parallel and perpendicular polarized light. The data were analyzed according to the theory of site-specific infrared dichroism described previously (Arkin et al. 1997).

Global Search Molecular Dynamics (GSMD) protocol

The simulations were performed using a Compaq Alpha Cluster SC45, which contains 47 nodes. All calculations were carried out using the parallel version of the molecular modeling and manipulation program, the Crystallography and NMR System (CNS Version 3.3), and the Parallel Crystallography and NMR System (PCNS) (Brunger et al. 1998). Using the OPLS (Optimized Potential for Liquid Simulations force field) (Jorgensen and Tirado-Rives 1988), the global search was carried out in vacuo with united atom topology, explicitly describing only polar and aromatic hydrogen atoms as described elsewhere (Adams et al. 1995) and using CHI 1.1 (CNS Helical Interactions) to obtain the initial configurations. The homo-oligomeric interaction between the helices was assumed to be symmetrical.

The protocol for the global search has been described previously. Briefly, trials were carried out starting from either left or right crossing angle configurations. The initial helix tilt, β , was restrained to 5° and the helices were rotated about their long helical axes in 10° increments until the rotation angle reached 350° . Henceforth, the simulation was repeated by increasing the helix tilt in discrete steps of 10° , up to 45° . We must note that the restraint for the helix tilt is not completely strict, i.e., at the end of the simulation a drift of up to $\pm 5^\circ$ from the initial restrained value could be observed in some cases. Three trials were carried out for each starting configuration using different initial random velocities, for right- and left-handed configurations, and only for pentamers, for all 13 sequences, totaling 13,650 structures. Clusters were identified for each tilt with a minimum number of similar structures. Any structure belonging to a certain cluster was within 1.0 Å RMSD from any other structure within the same cluster. Finally, the structures belonging to each cluster were averaged and subjected to energy minimization. These final averaged structures, with a certain tilt and rotational orientation, were taken as the representatives of the respective clusters.

Intersequence comparisons between clusters were performed by calculating the RMSD between their α -carbon backbone using the program ProFit (<http://www.bioinf.org.uk/software/profit>). The structure preserved in sequences was taken as the likely model of interaction.

Homologous sequences for SH

A total of 13 sequences were used for the simulations (Fig. 2). Homologous sequences were obtained using ncbi homoloGene search (<http://www.ncbi.nlm.nih.gov/>). The assignment of the transmembrane domain for these sequences was based on the hydrophilicity/surface probability plots (Krogh et al. 2001) and the transmembrane predictions from the TMHMM server (Sonnhammer et al. 1998). According to these predictors, the transmembrane region of these sequences spans 23 residues. The alignment of these sequences in the TM domain is shown in Figure 2, with their NCBI accession numbers shown in the left column.

Ion channel recording

Ion channel formation of SH-TM was measured by single channel recording. A bilayer membrane was formed on a 250- μ m (or 150- μ m) septum of a Delrin cup with a working volume of 1 mL in each *cis* and *trans* chamber. Single channel experiments were carried out in asymmetric ionic conditions. The *cis* and *trans* chambers consist of 500 mM NaCl, 50 mM HEPES, pH 7.2, and 50 mM NaCl and 50 mM of HEPES, pH 7.2, respectively. A lipid cocktail of POPE:POPS:POPC (5:3:2, v/v/v) and a lipid concentration of 50 mg/mL were used to form the artificial lipid bilayer. The lipid cocktail was painted onto the hole of the Delrin cup. Usually the bilayer could be formed quickly in the presence of asymmetric solution. The bilayer formation was examined electrically by the current amplitude when a voltage pulse was applied.

The whole assembly was shielded from electrical and vibration interference. After the formation of the bilayer across the aperture of the septum, small aliquots of SH-TM (~5–10 μ g) reconstituted in liposome were added to the *cis* chamber with continuous stirring to facilitate the insertion of the peptide into the planar lipid bilayer. Stirring of the solution was stopped

when channel activity was detected. Electrical currents were recorded using a Bilayer Clamp BC-525D amplifier (Warner Instruments) in capacitive feedback configuration via Ag/AgCl electrodes linked via agar salt bridges (2% of agarose in 1 M NaCl). The *trans* chamber was set as reference and the *cis* chamber was held at different potentials ranging from -100 mV to $+20$ mV in 20-mV increments. Data were filtered at 50 Hz with an 8-pole Bessel filter, and analog output signal was digitized at a sampling rate of 1 kHz by using an A/D converter (Digidata 1322A, Axon Instruments). Data processing was performed using pClamp 9.2 software (Axon Instruments). Single channel conductance was calculated from the corresponding Gaussian fits using SigmaPlot 9.0 software (Systat Software, Inc.) to current histograms by using data from segments of continuous recordings lasting longer than 10 s. Openings shorter than 0.5 ms were ignored. To avoid electrostatic interference during recording, the recording cells were placed in a Faraday cage set on a mechanically isolated table to obtain low-noise recording of single channel currents. Data were recorded at room temperature. Voltages were corrected for calculated liquid junction potential using pClamp 9.2 software (Axon Instruments).

Acknowledgments

J.T. thanks the Ministry of Education and the Biomedical Research Council of Singapore for financial support, grants ARC 7/05 and 04/1/22/19/361, respectively.

References

- Adams, P.D., Arkin, I.T., Engelman, D.M., and Brunger, A.T. 1995. Computational searching and mutagenesis suggest a structure for the pentameric transmembrane domain of phospholamban. *Nat. Struct. Biol.* **2**: 154–162.
- Arkin, I.T., MacKenzie, K.R., and Brunger, A.T. 1997. Site-directed dichroism as a method for obtaining rotational and orientational constraints for oriented polymers. *J. Am. Chem. Soc.* **119**: 8973–8980.
- Baker, E.N. and Hubbard, R.E. 1984. Hydrogen bonding in globular proteins. *Prog. Biophys. Mol. Biol.* **44**: 97–179.
- Ballesteros, J.A., Deupi, X., Olivella, M., Haaksma, E.E.J., and Pardo, L. 2000. Serine and threonine residues bend α -helices in the $\chi_1 = g$ -conformation. *Biophys. J.* **79**: 2754–2760.
- Beevers, A.J. and Kukol, A. 2006. Secondary structure, orientation, and oligomerization of phospholemman, a cardiac transmembrane protein. *Protein Sci.* **15**: 1127–1132.
- Boonserm, P., Moonsom, S., Boonchoy, C., Promdonkoy, B., Parthasarathy, K., and Torres, J. 2006. Association of the components of the binary toxin from *Bacillus sphaericus* in solution and with model lipid bilayers. *Biochem. Biophys. Res. Commun.* **342**: 1273–1278.
- Briggs, J.A.G., Torres, J., and Arkin, I.T. 2001. A new method to model membrane protein structure based on silent amino acid substitutions. *Proteins: Struct., Funct., Genet.* **44**: 370–375.
- Brunger, A.T., Adams, P.D., Clore, G.M., DeLano, W.L., Gros, P., Grosse-Kunstleve, R.W., Jiang, J.S., Kuszewski, J., Nilges, M., Pannu, N.S., et al. 1998. Crystallography & NMR system: A new software suite for macromolecular structure determination. *Acta Crystallogr., Sect. D: Biol. Crystallogr.* **54**: 905–921.
- Bukreyev, A., Whitehead, S.S., Murphy, B.R., and Collins, P.L. 1997. Recombinant respiratory syncytial virus from which the entire SH gene has been deleted grows efficiently in cell culture and exhibits site-specific attenuation in the respiratory tract of the mouse. *J. Virol.* **71**: 8973–8982.
- Burg, E.D., Remillard, C.V., and Yuan, J.X.J. 2006. K^+ channels in apoptosis. *J. Membr. Biol.* **209**: 3–20.
- Byler, D.M. and Susi, H. 1986. Examination of the secondary structure of proteins by deconvolved FTIR spectra. *Biopolymers* **25**: 469–487.
- Collins, P.L. and Mottet, G. 1993. Membrane orientation and oligomerization of the small hydrophobic protein of human respiratory syncytial virus. *J. Gen. Virol.* **74**: 1445–1450.

- Cymes, G.D., Ni, Y., and Grosman, C. 2005. Probing ion-channel pores one proton at a time. *Nature*. **438**: 975–980.
- Duff, K.C. and Ashley, R.H. 1992. The transmembrane domain of influenza A M2 protein forms amantadine-sensitive proton channels in planar lipid bilayers. *Virology* **190**: 485–489.
- Fuentes, S., Tran, K.C., Luthra, P., Teng, M.N., and He, B. 2007. Function of the respiratory syncytial virus small hydrophobic protein. *J. Virol.* **81**: 8361–8366.
- Gan, S.W., Xin, L., and Torres, J. 2007. The transmembrane homotrimer of ADAM 1 in model lipid bilayers. *Protein Sci.* **16**: 285–292.
- Gonzalez, M.E. and Carrasco, L. 2003. Viroporins. *FEBS Lett.* **552**: 28–34.
- Gratkowski, H., Lear, J.D., and DeGrado, W.F. 2001. Polar side chains drive the association of model transmembrane peptides. *Proc. Natl. Acad. Sci.* **98**: 880–885.
- Griffin, S.D., Beales, L.P., Clarke, D.S., Worsfold, O., Evans, S.D., Jaeger, J., Harris, M.P., and Rowlands, D.J. 2003. The p7 protein of hepatitis C virus forms an ion channel that is blocked by the antiviral drug, Amantadine. *FEBS Lett.* **535**: 34–38.
- Heminway, B.R., Yu, Y., Tanaka, Y., Perrine, K.G., Gustafson, E., Bernstein, J.M., and Galinski, M.S. 1994. Analysis of respiratory syncytial virus F, G, and SH proteins in cell fusion. *Virology* **200**: 801–805.
- Jorgensen, W.L. and Tirado-Rives, J. 1988. The OPLS (optimized potentials for liquid simulations) potential functions for proteins, energy minimizations for crystals of cyclic peptides and crambin. *J. Am. Chem. Soc.* **110**: 1657–1666.
- Kochva, U., Leonov, H., and Arkin, I.T. 2003. Modeling the structure of the respiratory syncytial virus small hydrophobic protein by silent-mutation analysis of global searching molecular dynamics. *Protein Sci.* **12**: 2668–2674.
- Kovacs, F.A. and Cross, T.A. 1997. Transmembrane four-helix bundle of influenza A M2 protein channel: Structural implications from helix tilt and orientation. *Biophys. J.* **73**: 2511–2517.
- Krogh, A., Larsson, B., von Heijne, G., and Sonnhammer, E.L.L. 2001. Predicting transmembrane protein topology with a hidden Markov model: Application to complete genomes. *J. Mol. Biol.* **305**: 567–580.
- Lang, F., Foller, M., Lang, K.S., Lang, P.A., Ritter, M., Gulbins, E., Vereninov, A., and Huber, S.M. 2005. Ion channels in cell proliferation and apoptotic cell death. *J. Membr. Biol.* **205**: 147–157.
- Lin, X., Tan, S.M., Law, S.K.A., and Torres, J. 2006. Two types of transmembrane homomeric interactions in the integrin receptor family are evolutionarily conserved. *Proteins* **63**: 16–23.
- Okada, A., Miura, T., and Takeuchi, H. 2001. Protonation of histidine and histidine-tryptophan interaction in the activation of the M2 ion channel from influenza A virus. *Biochemistry*. **40**: 6053–6060.
- Olmsted, R.A. and Collins, P.L. 1989. The 1A protein of respiratory syncytial virus is an integral membrane protein present as multiple, structurally distinct species. *J. Virol.* **63**: 2019–2029.
- Perez, M., García-Barreno, B., Melero, J.A., Carrasco, L., and Guinea, R. 1997. Membrane permeability changes induced in *Escherichia coli* by the SH protein of human respiratory syncytial virus. *Virology* **235**: 342–351.
- Ramjeesingh, M., Huan, L.J., Garami, E., and Bear, C.E. 1999. Novel method for evaluation of the oligomeric structure of membrane proteins. *Biochem. J.* **342**: 119–123.
- Rixon, H.W., Brown, G., Aitken, J., McDonald, T., Graham, S., and Sugrue, R.J. 2004. The small hydrophobic (SH) protein accumulates within lipid-raft structures of the Golgi complex during respiratory syncytial virus infection. *J. Gen. Virol.* **85**: 1153–1165.
- Rixon, H.W., Brown, G., Murray, J.T., and Sugrue, R.J. 2005. The respiratory syncytial virus small hydrophobic protein is phosphorylated via a mitogen-activated protein kinase p38-dependent tyrosine kinase activity during virus infection. *J. Gen. Virol.* **86**: 375–384.
- Skehel, J.J. 1992. Influenza virus. Amantadine blocks the channel. *Nature* **358**: 110–111.
- Smith, S.O., Eilers, M., Song, D., Crocker, E., Ying, W., Groesbeck, M., Metz, G., Ziliox, M., and Aimoto, S. 2002. Implications of threonine hydrogen bonding in the glycophorin A transmembrane helix dimer. *Biophys. J.* **82**: 2476–2486.
- Sonnhammer, E.L., von Heijne, G., and Krogh, A. 1998. A hidden Markov model for predicting transmembrane helices in protein sequences. *Proc. Int. Conf. Intell. Syst. Mol. Biol.* **6**: 175–182.
- Szabo, I., Adams, C., and Gulbins, E. 2004. Ion channels and membrane rafts in apoptosis. *Pflugers Arch.* **448**: 304–312.
- Tamm, L.K. and Tatulian, S.A. 1997. Infrared spectroscopy of proteins and peptides in lipid bilayers. *Q. Rev. Biophys.* **30**: 365–429.
- Techaarpornkul, S., Barretto, N., and Peebles, M.E. 2001. Functional analysis of recombinant respiratory syncytial virus deletion mutants lacking the small hydrophobic and/or attachment glycoprotein gene. *J. Virol.* **75**: 6825–6834.
- Therien, A.G. and Deber, C.M. 2002. Oligomerization of a peptide derived from the transmembrane region of the sodium pump γ subunit: Effect of the pathological mutation G41R. *J. Mol. Biol.* **322**: 583–590.
- Torres, J., Adams, P.D., and Arkin, I.T. 2000. Use of a new label, $^{13}\text{C}=^{18}\text{O}$, in the determination of a structural model of phospholamban in a lipid bilayer. Spatial restraints resolve the ambiguity arising from interpretations of mutagenesis data. *J. Mol. Biol.* **300**: 677–685.
- Torres, J., Kukol, A., and Arkin, I.T. 2001a. Mapping the energy surface of transmembrane helix-helix interactions. *Biophys. J.* **81**: 2681–2692.
- Torres, J., Kukol, A., Goodman, J.M., and Arkin, I.T. 2001b. Site-specific examination of secondary structure and orientation determination in membrane proteins: The peptidic $^{13}\text{C}=^{18}\text{O}$ group as a novel infrared probe. *Biopolymers* **59**: 396–401.
- Torres, J., Briggs, J.A.G., and Arkin, I.T. 2002. Contribution of energy values to the analysis of global searching molecular dynamics simulations of transmembrane helical bundles. *Biophys. J.* **82**: 3063–3071.
- Torres, J., Wang, J., Parthasarathy, K., and Liu, D.X. 2005. The transmembrane oligomers of coronavirus protein E. *Biophys. J.* **88**: 1283–1290.
- Torres, J., Maheswari, U., Parthasarathy, K., Ng, L., Lu, D.X., and Gong, X. 2007. Conductance and amantadine binding of a pore formed by a lysine-flanked transmembrane domain of SARS coronavirus envelope protein. *Protein Sci.* **16**: 2065–2071.
- Wellings, D.A. and Atherton, E. 1997. Standard Fmoc protocols. *Methods Enzymol.* **289**: 44–67.
- Whitehead, S.S., Bukreyev, A., Teng, M.N., Firestone, C.Y., St. Claire, M., Elkins, W.R., Collins, P.L., and Murphy, B.R. 1999. Recombinant respiratory syncytial virus bearing a deletion of either the NS2 or SH gene is attenuated in chimpanzees. *J. Virol.* **73**: 3438–3442.